Phys. Lett. B 859 (2024) 139087

Contents lists available at ScienceDirect

Physics Letters B

journal homepage: www.elsevier.com/locate/physletb

Letter

Quenching of the quantum *p*-strength in light exotic nuclei

E. Cravo [a,b], R.B. Wiringa [c], R. Crespo [d,e,*], A. Arriaga [b], A. Deltuva [f], M. Piarulli [g,h]

[a] Centro de Física Teórica e Computacional, Faculdade de Ciências, Universidade de Lisboa, Campo Grande, 1749-016 Lisboa, Portugal
[b] Departamento de Física, Faculdade de Ciências, Universidade de Lisboa, Campo Grande, 1749-016 Lisboa, Portugal
[c] Physics Division, Argonne National Laboratory, Argonne, IL 60439, USA
[d] Departamento de Física, Instituto Superior Técnico, Universidade de Lisboa, Av. Rovisco Pais 1, 1049-001, Lisboa, Portugal
[e] Centro de Ciências e Tecnologias Nucleares, Universidade de Lisboa, Estrada Nacional 10, 2695-066 Bobadela, Portugal
[f] Institute of Theoretical Physics and Astronomy, Vilnius University, Saulėtekio al. 3, LT-10257 Vilnius, Lithuania
[g] Department of Physics, Washington University in Saint Louis, Saint Louis, MO 63130, USA
[h] McDonnell Center for the Space Sciences at Washington University in St. Louis, MO 63130, USA

ARTICLE INFO

Editor: A. Schwenk

Keywords:
Many-body *ab initio* structure
Few-body reaction
(p,pN) reactions

ABSTRACT

One-nucleon spectroscopic overlaps, their strength or spectroscopic factors (SFs), and nucleon removal cross sections for light nuclei in the mass range A≤ 12 were evaluated using the fully correlated Quantum Monte Carlo (QMC) wave functions (WFs). Harder (AV18+UX) and softer (NV2+3) bare interactions were used providing consistent results. The SFs were also taken from simple Shell Model (SM) calculations. This structure information was incorporated in the standard three-body Faddeev/Alt-Grassberger-Sandhas reaction formalism to evaluate the (p,pN) cross sections. The results further our understanding of the quenching of the quantum *p*-shell strength obtained from structure and reactions. We have found the ratios of the total QMC sums of SFs to the SM ones to be uniform and ∼ 3/4. The corresponding ratios of the sums Below Particle Threshold (BPT) of SFs, as well as of total cross sections, deviate strikingly from the uniform trend in some special cases. We find these ratios to be close to unit for ^{9}Li →^{8} Li + n and ^{9}C →^{8} B + p. In contrast, they are strongly reduced for ^{11}C →^{10} C + n and ^{11}B →^{10} Be + p mirror transitions, resulting from the quenching of the strength for low-lying 2^{+} final state transitions. The QMC theoretical cross section BPT for ^{11}C(p,pn) is about two times smaller than the experimental data.

1. Introduction

The study of light systems is of prime importance for the understanding of both primordial and stellar nucleosynthesis. During the nuclear synthesis, nucleons (N) organize themselves and build a large variety of complex nuclei with intriguing phenomena, such as the coexistence of single-particle states and collective modes, and the occurrence of critically low thresholds for particle/cluster emission near the ground state, in both heavy and light systems. This ultimately traces back to the complexity of bare NN and NNN interactions that are responsible for the evolution of the nuclear landscape. These bare interactions induce important correlations, in particular NN correlations in nuclear medium, such as short-ranged and tensor.

Nuclear correlations have been interpreted as responsible for the breakdown of simple independent shell model (SM) descriptions of nuclei, as seen for example in the quenching of single-particle strength obtained from both state-of-the-art structure models and direct reactions with stable and rare-isotope beams and electron or nuclear probes. In particular, it was found that the theoretical total cross sections calculated from simple shell model exceed the experimental data [1–12,14,13,15–17]. Nevertheless, the origin and the behaviour of reduction patterns along the nuclear landscape remain a longstanding puzzle. These analyses made use of different probes, energy regimes, and a panoply of reaction and structure models. In particular some focus on observables that probe not only the nuclear surface but also its interior, while others just sample the nuclear surface. Clearly, the fingerprints and the driving mechanisms of nuclear correlations need to be identified consistently and unambiguously as well as understood from first principles, ultimately using full many-body approaches.

In this manuscript, we make a comprehensive analysis of the nucleon knockout reactions, $^{A}\mathrm{P} \rightarrow {}^{A-1}\mathrm{R} + \mathrm{N}$, for a variety of light exotic systems within the mass range A ≤ 12 represented in Fig. 1. The detailed study

* Corresponding author at: Departamento de Física, Instituto Superior Técnico, Universidade de Lisboa, Av. Rovisco Pais 1, 1049-001, Lisboa, Portugal.
E-mail address: raquel.crespo@tecnico.ulisboa.pt (R. Crespo).

https://doi.org/10.1016/j.physletb.2024.139087
Received 30 July 2024; Received in revised form 9 October 2024; Accepted 17 October 2024
Available online 21 October 2024

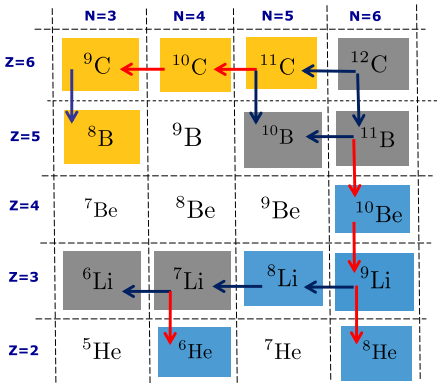

Fig. 1. Mapping of the light-nuclei landscape through (p,pN) reactions where the red arrows represent the knockout of a deficient species nucleon.

of these knockout reactions has been made possible by recent advances in radioactive ion beam facilities and recent theoretical advances in the many-body theory. It includes cases of current interest such as the removal of a loosely bound and deficient (minority) species nucleon from the parent nucleus.

We deduce the quenching of the quantum *p*-shell spectroscopic strength obtained from *ab initio* structure calculations of the many-body wave functions, and from merging these into state-of-the-art few-body reaction theory for (p,pN) reactions, often coined as quasifree scattering.

We aim to answer two key questions: (i) Can the quenching of the quantum *p*-shell spectroscopic strength obtained from both state-of-the-art structure models and direct reactions with stable and rare-isotope beams and electron or nuclear probes be conciliated? (ii) Can key observables from (p,pN) reactions provide unequivocal information about nuclear spectroscopy, testing structure models and their underlying interactions?

In this analysis, *ab initio* wave functions are generated by solving the Schrödinger equation for the many-body system of protons and neutrons using quantum Monte Carlo (QMC) techniques for nuclear physics with full account of the complexity of the many-body spin- and isospin-dependent correlations induced by nuclear interactions. Among these are the variational Monte Carlo (VMC) and the Green's function Monte Carlo (GFMC). We make use of the Argonne v18 two-nucleon and Urbana X three-nucleon potentials (AV18+UX) designed and fine-tuned so that they are able to reproduce two-, three-, and four-nucleon data with high accuracy [19–21]. Additionally, we use the Norfolk NV2+3 Δ-full local chiral effective field theory (χEFT) interactions (NV2+3-Ia, -Ia*, and -IIb*) that use low-energy constants constrained to reproduce NN scattering data and trinucleon properties [26–28]. These potentials range from a version with a fairly 'hard' repulsive core (AV18+UX) to a version with a fairly 'soft' core (NV2+3-Ia). The calculated QMC one-body momentum distributions have a maximum at or near k = 0 fm^{-1}, a rapid fall off at k$\sim$ 2 fm^{-1}, followed by a high-momentum tail that is more prominent for hard interactions, and less so for softer ones [28]. The use of multiple microscopic potentials begins to give an idea of the theoretical uncertainty associated with choice of interaction. Although the chiral potentials are derived from more fundamental grounds, only the very short-range repulsive core shows significant differences with the AV18+UX interaction; the less repulsive core of the NV2+3-Ia induces softer short-range correlations in the QMC wave functions. It is well known that the repulsive core, and its corresponding correlations, is indeed one of the major uncertainties of the nuclear interaction, so attempts to improve our understanding are important and timely. Our results show, however, that the observables in the type of reaction under study here are not very sensitive to these differences in the QMC wave functions.

The QMC methods have been used to study a wide mass range of nuclear systems. The VMC and GFMC methods have been used extensively for A$\leq$12 nuclei, while a cluster VMC (CVMC) has been used for A = 16,40 calculations. Another variant, auxiliary field diffusion Monte Carlo (AFDMC) has been used for dense nuclear and neutron matter for astrophysics applications such as neutron stars [21,25]. These methods have successfully described fundamental nuclear properties of light nuclei such as the energy levels, level ordering, and radii of nuclei in the mass range A = 4–12 in very satisfactory agreement with experimental data [26], as well as the relative stability of light nuclei, including the absence of particle-stable A = 5,8 nuclei. The QMC WFs are also able to predict the appearance of clusterization phenomena [19,21,22]. In other words, the QMC methods have the ability to capture simultaneously single-particle-like and highly-correlated states. This feature is completely absent in standard shell model approaches as for example the one proposed by Cohen and Kurath [23].

The one-nucleon knockout reactions, from a parent nucleus, ^{A}P, leading to the daughter or residue, $^{A-1}$R, in the ground or any excited state, have been widely used to explore the single-particle components of a nucleus [6–17]. At intermediate and high-energy regimes, it is standardly assumed that the probe knocks a single nucleon without large momentum transfer to the residual nucleus which participates as a spectator during the reaction process. Then, under this crucial assumption, the two-body partition for the vertex between the initial and residual nucleus selects a particular core-valence component in the initial nucleus. As a result, the one-nucleon spectroscopic overlap (SO) defined as a projection of a parent state onto an antisymmetrized core-valence form becomes a key structure input for the reaction formalism [15,18]. This overlap takes into account all the possible many-body partitions of the parent nucleus beyond the $^{A-1}$R + N configuration. For a given state of the residual nucleus, the one-nucleon spectroscopic overlap is a superposition of different nucleon angular momentum channels, ℓj, satisfying the appropriate triangular relations [18]. The strength of the overlap, or the so called spectroscopic factor (SF), for a given transition is obtained from the integral of the one-nucleon overlap function in each angular momentum channel.

When a p-orbital spin-1/2 nucleon is removed from an A-body nucleus, the spectroscopic overlaps are controlled by three simple rules that apply to the spin-space symmetry components of a state: $^{(2S+1)}$L$[sp_xp_yp_z]$ where S is the total spin of the nucleons, L is the orbital angular momentum, and $[sp_xp_yp_z]$ is the Young label for the spatial symmetry, with a maximum value of 4 spin-isospin states in each of the s, p_x, p_y, and p_z orbitals [22]. The dominant spin-space symmetry components for the ground and excited states of selected light nuclei considered here are shown in Fig. 2. The simple rules are that S changes by one unit, L can change by 0,±1, and $[sp_xp_yp_z]$ decreases by one unit, e.g., a [43] space component can reduce to [42] but not to [411]. This is illustrated in Fig. 2, where the ^{11}B ground state with [443] symmetry has significant overlap with the ^{10}Be 0^+ ground state and first two 2^+ excited states that have [442] symmetry, as well as some higher-lying [433] states, but not to intermediate [4411] states.

The QMC one-nucleon spectroscopic overlaps are incorporated in the state-of-the-art Faddeev/Alt-Grassberger-Sandhas (F/AGS) approach to solve the resulting three-body scattering problem [37,38]. The F/AGS allows a consistent and simultaneous treatment of all open channels, providing an exact solution of the three body scattering problem for an assumed three-body Hamiltonian. This formalism includes all multiple scattering terms, contrary to other scattering frameworks that rely on assumed exact cancellations between multiple scattering terms [14]. It has been used recently in several exploratory studies of (p,pN) reactions [8,13–15].

2. Results and discussion

The root-mean-square (rms) charge radius of a nucleus is a crucial observable [29] that reflects important nuclear structure changes,

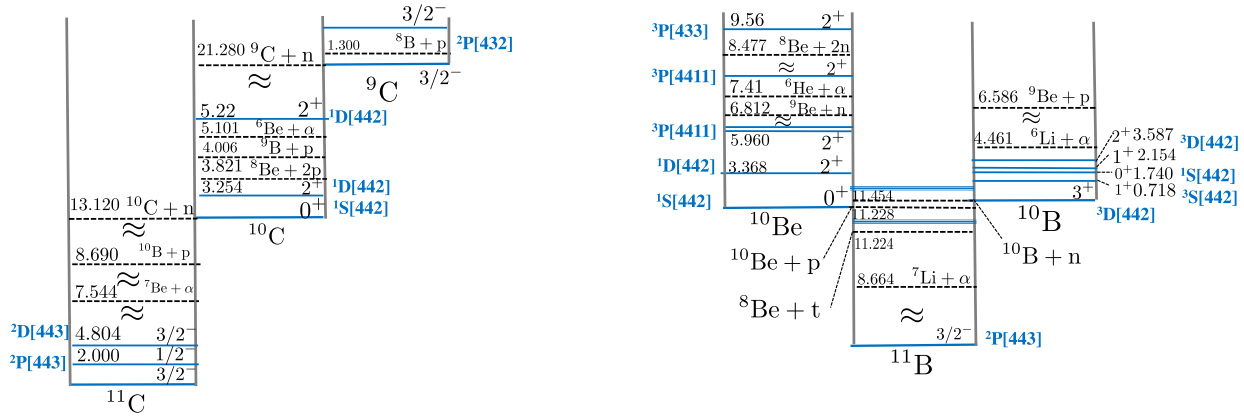

Fig. 2. Energy spectrum of selected nuclei including the low-lying particle thresholds and the dominant spin-space symmetry components of the ground and excited states.

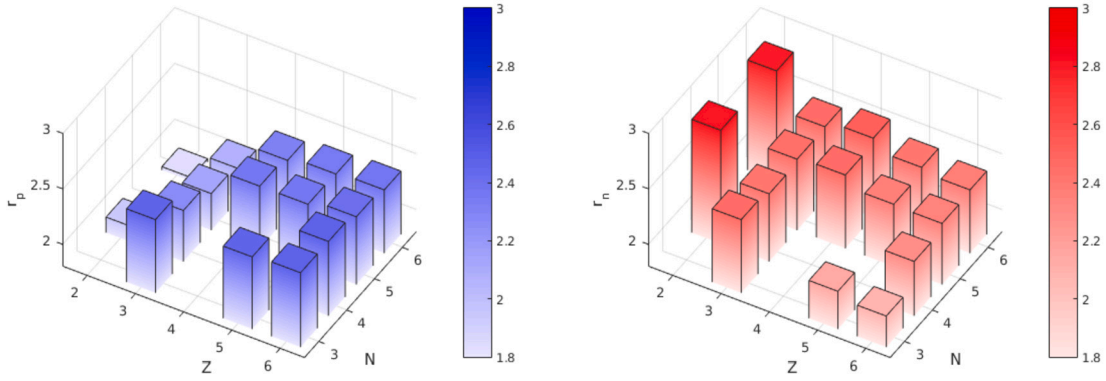

Fig. 3. Isotopic and isotonic distribution of the QMC point proton (left) and neutron (right) rms radii.

for example, the occurrence of new/disappearance of traditional magic numbers or the change in correlations due to neutron excess [30]. It has been used to benchmark structure models in comparison with accurate measurements [31]. We have found quite a reasonable agreement of the VMC point proton rms radii of the studied nuclei with the very accurately calculated GFMC values and the experimental [32,33] ones (shown in Table 2 of Supplemental material), validating the VMC approach. The experimental values for point proton rms radii are obtained from measured charge radii by making standard adjustments for finite proton and neutron size effects and relativistic and spin-orbit corrections, as discussed in [33].

The isotopic and isotonic distributions of the point proton and neutron rms radii are shown in Fig. 3. The helium isotopes have an α-like core that changes relatively little going from $A=4$ to 6 and 8 (as indicated by two-proton density distributions), while the loosely-bound p-shell neutrons are correlated to one side, thus altering the center of mass and significantly increasing the single-proton radii from ^{4}He. For the case of the neutron-rich lithium chain, the one p-shell proton increases the single-proton distribution significantly compared to helium, but gradually becomes more compact as neutrons are added, while the neutron distribution increases slowly. For the carbon chain, the inverse happens, i.e., as neutrons are removed and binding decreases, the protons become slightly more diffuse.

We have obtained improved one-nucleon spectroscopic overlaps and theoretical SFs, with associated i transition quantum numbers, representing the final state spin of the residue, the nucleon orbital angular and total angular momenta (ℓ, j). We consider p-wave nucleon channels. These SFs were calculated from the fully correlated QMC WFs for the AV18+UX and NV2+3 interactions. The SFs from the simple SM of Cohen and Kurath (CK) were taken from Ref. [23]. For each model $\mathcal{M}$ we have obtained the total sum of SFs, $\Sigma(\mathcal{M}) = \Sigma_i Z^i(\mathcal{M})$ as shown in Table 3 of the Supplemental material. Tabulations and figures of the SOs and SFs are also available online [24].

The simple SM of CK makes use of a truncated nuclear state space, which assigns to one the probability of finding all valence nucleons in p-shells in the parent and residual nuclei and the $(A-1)+N$ configuration in the parent nucleus. As a result, the SFs (before the c.m. correction) for all the transitions here presented exhaust the sum rule (with the exception of ^{9}C $\rightarrow^8$ B + p). The *ab initio* QMC wave functions are constructed starting from a complete p-shell single-particle basis, so there is a one-to-one correspondence between the CK and QMC states. For example, ^{7}Li with one valence proton in the p-shell, has p-wave spectroscopic overlaps with five spin-parity levels (0^+,2^+,2^+,1^+,0^+) in ^{6}He. With CK the SFs add up to 1.00, while the correlated QMC wave functions for the same set of states give 0.73 for the 'hard' AV18+UX phenomenological interaction and 0.81 for the 'soft' NV2+3-Ia chiral interaction. We attribute this quenching of SF strength to the microscopic correlations in the QMC wave functions that include the equivalent of extensive multi-particle, multi-shell excitations in a harmonic oscillator framework, effectively pushing particles out of the p-shell. Thus with these correlated wave functions, the sum of p-shell strength for the same states as CK does not exhaust the sum rule.

Additionally, we have evaluated the partial sums for which the experimental energy of the daughter nucleus resides Below Particle Threshold (BPT), $\Sigma_{\rm BPT}$ (collected in Table 3 of the Supplemental material), i.e., states below particle emission of the daughter nucleus. Although the coupling to the continuum is not considered explicitly, the physics information contained in these sums includes the effect of many-body configurations that shift strength from BPT to higher excited states above threshold and in the continuum. This missing strength could include, e.g., fragmentation of the daughter into multiple clusters, which would have an overlap with the parent ground state wave function.

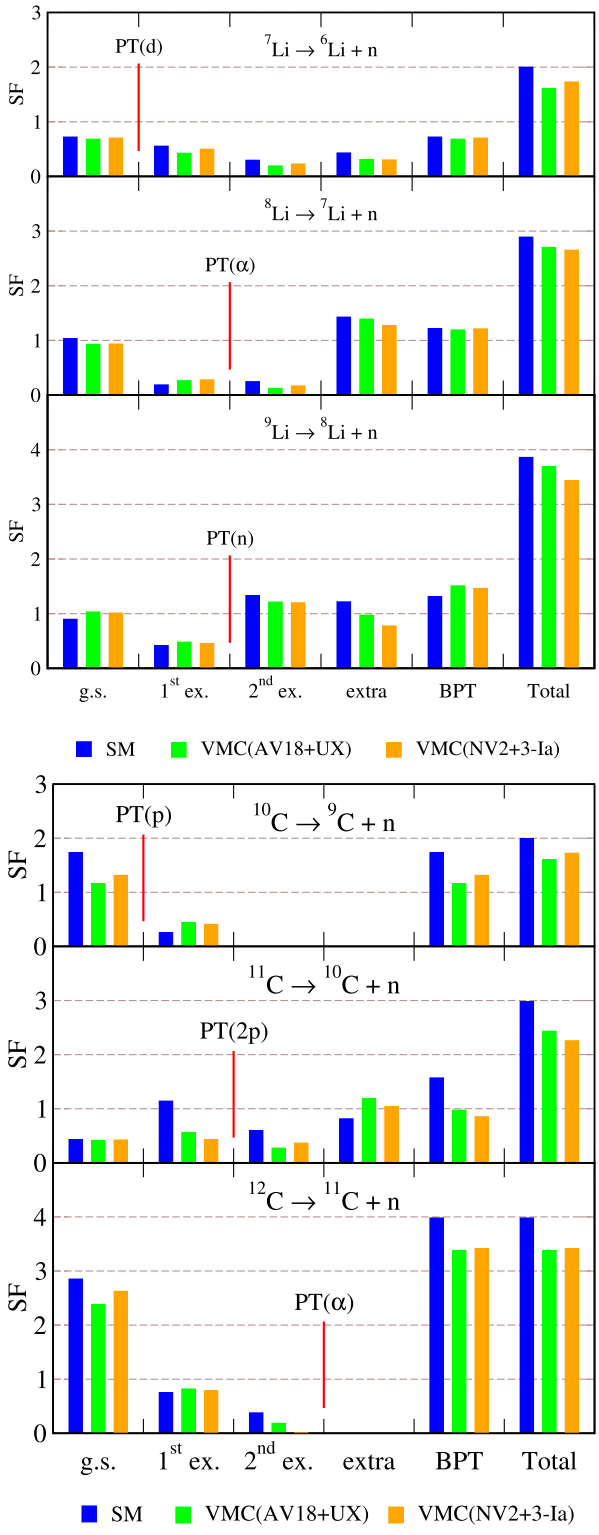

Fig. 4. Representation of the SFs and their sums (BPT and total) for selected n-removal transitions taken from QMC with the AV18+UX and NV2+3-Ia bare interactions and simple Shell Model (SM) calculations. The particle threshold (PT) of the residue is indicated.

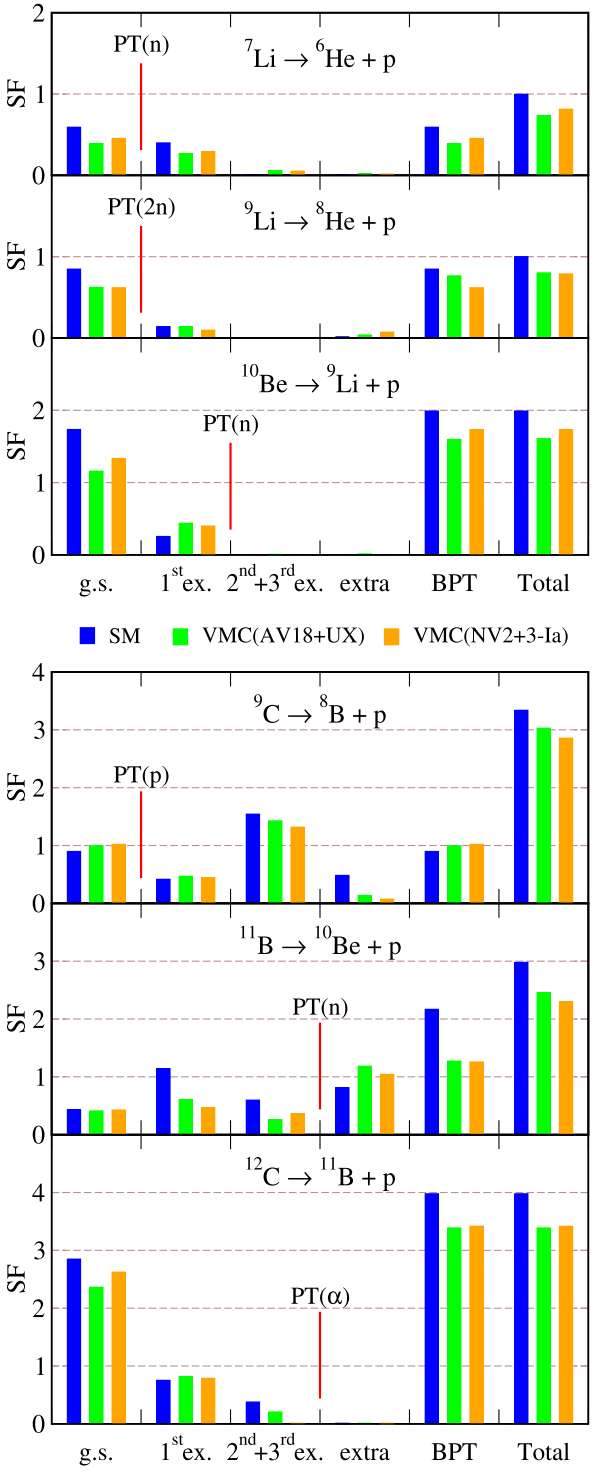

Fig. 5. Representation of the SFs and their sums (BPT and total) for selected p-removal transitions taken from QMC with the AV18+UX and NV2+3-Ia bare interactions and simple Shell Model (SM) calculations. The particle threshold (PT) of the residue is indicated.

In Figs. 4 - 5 we represent the SFs and their sums (BPT and total) for selected transitions taken from Table 3. Overall, we find that the total SF sums evaluated from the SM follow the expected trend of being relatively larger than the QMC ones. Nevertheless, the relative distribution of the strength might vary between the ground, excited and continuum final states.

The cases where VMC predicts the greatest quenching relative to the CK SM are the mirror transitions ^{11}C→^{10}C + n and ^{11}B → ^{10}Be + p with a (2p)/(1n) PT of the residue respectively. As seen in Table 3 (and depicted in Figs. 4 - 5), the parent to daughter ground state SFs are very similar, but SFs to the daughter low-lying excited states (which

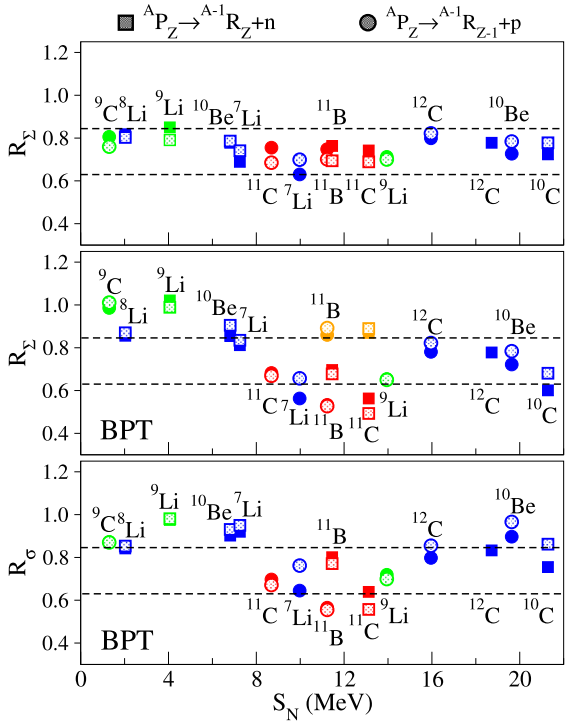

Fig. 6. Theoretical (QMC/SM) ratios as functions of the nucleon separation energy: total sums of SFs (upper panel), sums of SFs restricted to final states BPT of the residual nucleus (middle panel), and total (p,pN) cross sections BPT (lower panel). Results are calculated using the AV18+UX (filled symbols) and NV2+3-Ia (dotted symbols) interactions. The transitions to the ground state are depicted in orange for the cases that significantly differ from those BPT.

have a much bigger SF) are highly quenched. These 2^+ excited states are strongly clustered in VMC, with a deformed ^{8}Be core, which may be very hard for a spherical SM to represent. This relative quenching is also in agreement with the SM obtained from the OXBASH code using the WBT interaction in the *spsdpf* model space restricted to $(0+1)\hbar\omega$ [11]. This reduction of the 2^+ strength is redistributed to higher excited states above threshold and in the continuum. For the $^{11}\mathrm{B} \rightarrow {}^{10}\mathrm{Be} + \mathrm{p}$ transition, we find the ratio of the VMC to the simple SM of the total 2^+ strength to be $\mathrm{R}_{2+} = 0.8$.

The cases with the least quenching relative to CK SM are the mirror transitions $^9\mathrm{Li} \rightarrow {}^8\mathrm{Li} + \mathrm{n}$ and $^9\mathrm{C} \rightarrow {}^8\mathrm{B} + \mathrm{p}$, where the ratio is near unity. The VMC wave functions for ^{9}Li and ^{9}C show the least clustering of all the nuclei studied in this work, and thus may be closer to a spherical SM representation. In fact, the VMC amplitudes for different spatial symmetries in ^{9}Li are remarkably close to those of the SM calculation by Kumar [43].

Despite the very different nature of the NV2+3 local chiral potentials and AV18+UX bare interactions, the total SF sums for the p-shell are fairly similar, usually within 5% for overlaps with the daughter ground states, although some of those with the daughter excited states can vary up to 10%.

The ratios of the total QMC sums of SFs, to the SM (CK) ones, (including c.m. correction for the SM) [44], $\mathrm{R}_\Sigma = \Sigma(\mathrm{QMC})/\Sigma(\mathrm{SM}^\dagger)$, are represented in the upper panel of Fig. 6 as a function of the nucleon separation energy, S_N of the parent nucleus which determines the fall of the overlap tail. For transitions to the ground state, the overlaps and consequently the SFs, were found to be determined by the interplay of this asymptotic behaviour with the difference between the removed nucleon rms radii, $\Delta r_N = r_N(A) - r_N(A-1)$ [15]. However, the results shown here are independent of the representation.

These ratios are roughly constant, ranging in the interval [0.65, 0.85], that is, about $\sim 3/4$ consistently with Refs. [39,40]. The results are similar to those obtained from (e,e′p) experiments across the nuclear chart and for stable nuclei, and transitions to the ground-state, showing a uniform quenching to 60-70% of the Independent Particle Model [1,2]. As mentioned above, the quenching of the total sum of SFs is fairly independent of the underlying bare interaction, harder (AV18+UX), represented by filled symbols, or a softer (NV2+3) one, represented by dotted symbols.

The ratios of SFs summed BPT, R_Σ(BPT), are represented in the middle panel of Fig. 6. These follow a fairly similar trend like R_Σ. However, as a result of SF quenching it deviates strongly in some special cases. While the ratios for transitions to the ground state resulting from N-removal from the mirror nuclei ^{11}C and ^{11}B follow the same trend, the mirror transitions $^{11}\mathrm{C} \rightarrow {}^{10}\mathrm{C} + \mathrm{n}$ and $^{11}\mathrm{B} \rightarrow {}^{10}\mathrm{Be} + \mathrm{p}$ are strongly quenched BPT due to the contribution of the transitions to the excited states. Moreover, these ratios BPT are close to unity for the mirror transitions $^9\mathrm{Li} \rightarrow {}^8\mathrm{Li} + \mathrm{n}$ and $^9\mathrm{C} \rightarrow {}^8\mathrm{B} + \mathrm{p}$. In the works of Refs. [34–36] it was also found, for other nuclei transitions, a departure from a constant trend.

The reaction observables for the (p,pN) reaction are calculated under the assumption that the residual nucleus is a spectator during the scattering process. In this case, the structure information for the reaction formalism is provided by the SOs, here deduced from QMC WFs. For each given state of the residual nucleus we have performed a convenient Woods-Saxon parametrization of these SOs that incorporates the adequate asymptotic behaviour, using the procedure described in Ref. [4,15,18]. This parametrization does not contain the Coulomb interaction, and considers a standard radius, diffuseness and depth adjusted to the separation energy of the removed nucleon. We use a standard diffuseness of $a = 0.65$ fm in all cases, except for ^{9}C in which case we take $a = 0.40$ fm, closer to a realistic description of the nucleus. After normalization to unity, the SOs are then incorporated in the three-body Faddeev/Alt-Grassberger-Sandhas (F/AGS) to get the single-particle cross sections.

For the three pair interactions required in the F/AGS reaction formalism, we take the realistic NN AV18 for the proton-nucleon pair and for the interactions between nucleons and the residual nucleus the non-relativistic reduction of the Cooper interaction [13,42] Koning and Delaroche (KD) OP parametrization [41] for the case of the Lithium isotopes. The uncertainty of the cross sections associated with optical parametrizations is estimated to be about 15% [14]. This is expected to be cancelled in the evaluation of theoretical ratios of cross sections. The theoretical inclusive cross section $\sigma_{\mathrm{th}}(\mathcal{M})$ is then obtained from the weighted sum of the theoretical SFs for a given structure model, $Z^i(\mathcal{M})$, and the single-particle cross sections, $\sigma^i_{\mathrm{sp}}(\mathcal{M})$, $\sigma_{\mathrm{th}}(\mathcal{M}) = \sum_i Z^i(\mathcal{M})\sigma^i_{\mathrm{sp}}(\mathcal{M})$, where the sum contains the states BPT. The calculated single particle cross sections are collected for representative examples in Table 4 of the Supplemental material. The relative difference corresponding to QMC overlaps calculated with softer and harder bare interactions was found to be less than ∼10%. These results indicate that cross sections probe essentially the on-shell behaviour of the NN transition amplitude and thus are fairly independent of the underlying NN interaction [15].

We have found that the single particle cross sections probe moderately the SO. Nevertheless, the theoretical ratios of the total cross sections BPT, $\mathrm{R}_\sigma(\mathrm{BPT}) = \sigma_{\mathrm{th}}(\mathrm{QMC})/\sigma_{\mathrm{th}}(\mathrm{SM}^\dagger)$, shown in the lower panel of Fig. 6 follow an identical dependence like R_Σ(BPT). They range in most cases in the interval [0.6 -0.85] compatible with the spectroscopic quenching obtained from (p,pN) reactions [7,8,10]. However, they are close to unit for $^9\mathrm{Li} \rightarrow {}^8\mathrm{Li} + \mathrm{n}$ and $^9\mathrm{C} \rightarrow {}^8\mathrm{B} + \mathrm{p}$, and strongly quenched for $^{11}\mathrm{C} \rightarrow {}^{10}\mathrm{C} + \mathrm{n}$ and $^{11}\mathrm{B} \rightarrow {}^{10}\mathrm{Be} + \mathrm{p}$ mirror transitions.

Lastly, we display in Table 1, the ratio of the partial sums of the cross sections taken from experimental data [11] to the theoretical results BPT, $R_S(\mathcal{M})$. The theoretical cross sections predict very well the experimental data for ^{12}C(p,pN), for both bare interactions. As expected, both SM calculations, performed with a truncated Hamiltonian, do over-estimate the data. On the other hand, for ^{11,10}C(p,pN) the QMC

Table 1
Ratio of the experimental partial sums of the cross sections [11] to the theoretical results BPT, $R_S(\mathcal{M})$, for different structure models and interactions.

Reaction	QMC			SM	
	AV18-UX	NV2+3-Ia	NV2+3-Ia*/ IIb*	CK	OXBASH [6,11]
^{12}C(p, 2p)^{11}B	0.90	0.79	0.99/0.84	0.72	0.60(6)(4)
^{12}C(p, pn)^{11}C	1.08	−−	−−	0.90	0.80(9)(7)
^{11}C(p, 2p)^{10}B	1.34	1.52	−−	0.92	0.86(4)(5)
^{11}C(p, pn)^{10}C	1.81	2.08	−−	0.96	1.06(9)(12)
^{10}C(p, pn)^{9}C	1.43	1.23	−−	1.08	0.99(13)(9)

underestimate the data while the SM results are fairly close to the data. This discrepancy is largest for the case of ^{11}C(p,pn)^{10}C, for which the QMC theoretical calculations underestimate the data by about a factor of two. This result, can be traced to the half predicted reduced p-shell strength BPT as compared to SM one. Contrary, the theoretical predictions based on the VMC wave functions overestimate the data by around a factor of two for the (^{7}Li, ^{6}He) and (^{10}Be, ^{9}Li) removal reactions of Ref. [4].

3. Summary and conclusions

The results obtained in this work represent progress toward a solution of the longstanding puzzle of reduction patterns obtained from structure and reactions along the nuclear landscape.

For light nuclei in the mass range A≤ 12 improved one-nucleon spectroscopic overlaps and their strengths or spectroscopic factors were evaluated from the fully correlated Quantum Monte Carlo wave functions with harder AV18+UX and softer NV2+3 interactions. The SFs were also taken from simple Shell Model calculations. This structure information was incorporated in the standard Faddeev/Alt-Grassberger-Sandhas reaction formalism to evaluate the (p,pN) cross sections assuming the residue to be inert during the scattering process.

The ratios of the total QMC sums of SFs, to the SM (CK) ones, are found to be essentially uniform, ranging in the interval [0.65, 0.85] that is ∼ 3/4. Noticeably, the ratios of the sums of SFs Below Particle Threshold deviate from this trend in special cases, being close to unit for ^{9}Li→^{8}Li + n and ^{9}C→^{8}B + p, and strongly reduced for ^{11}C→^{10}C + n and ^{11}B→^{10}Be + p mirror transitions. In the former, the VMC wave functions for ^{9}Li and ^{9}C show the least clustering of all the nuclei studied in this work, and are thus expected to be well described by a spherical SM representation. In the latter, while the parent to daughter ground state overlaps are very similar, the overlaps to the daughter low-lying 2^+ excited states (which have a much bigger SF) are highly quenched. The VMC predicts that these excited states are strongly clustered, with a deformed ^{8}Be core, and therefore expected to be poorly represented from spherical SM representation. Moreover, the quenching 2^+ strength is redistributed to higher excited states and into the continuum. The theoretical ratios of the total cross sections BPT probe moderately the SO, and thus exhibit a similar trend like the corresponding ratios of SFs.

The QMC theoretical cross section BPT for ^{11}C(p,pn) underestimates the data. The ratio of the cross sections taken from experimental data to the theoretical results BPT, R_S(QMC), is found to be about a factor of two. This discrepancy, not understood from the structure point of view, needs to be further investigated.

The above results are largely independent of the harder of softer character of the underlying bare interactions used in the QMC ab initio calculations.

For the understanding of nuclear correlations and its driving mechanisms, it would be very desirable to have a comprehensive N-knockout theoretical program, including the full merging of reactions and structure, and an experimental one with identification of the energy spectrum with high accuracy in the mass range A≤12.

Declaration of competing interest

The authors declare that they have no known competing financial interests or personal relationships that could have appeared to influence the work reported in this paper.

Acknowledgements

R.B.W. is supported by the US Department of Energy, Office of Nuclear Physics, contract No. DE-AC02-06CH11357, M.P. is supported by a 2021 Early Career Award number DE-SC0022002 and M.P. and R.B.W. are supported by the NUCLEI SciDAC program under award DE-SC0023495; computing time was provided by the Laboratory Computing Resource Center at Argonne National Laboratory. A.D. is supported by Lietuvos Mokslo Taryba (Research Council of Lithuania) under Contract No. S-MIP-22-72.

Appendix A. Supplementary material

Supplementary material related to this article can be found online at https://doi.org/10.1016/j.physletb.2024.139087.

Data availability

Data will be made available on request.

References

[1] L. Lápikas, Nucl. Phys. A 553 (1993) 297.
[2] G.J. Kramer, H. Blok, L. Lapikas, Nucl. Phys. A 679 (2001) 267.
[3] F. Flavigny, et al., Phys. Rev. Lett. 110 (2013) 122503.
[4] G.F. Grinyer, et al., Phys. Rev. C 86 (2012) 024315.
[5] J.A. Tostevin, A. Gade, Phys. Rev. C 90 (2014) 057602.
[6] V. Panin, et al., Phys. Lett. B 753 (2016) 204.
[7] L. Atar, et al., Phys. Rev. Lett. 120 (2018) 052501.
[8] P. Díaz Fernández, et al., Phys. Rev. C 97 (2018) 024311.
[9] S. Kawase, et al., Prog. Theor. Exp. Phys. 2018 (2018) 021D01.
[10] M. Gómez-Ramos, A.M. Moro, Phys. Lett. B 785 (2018) 511.
[11] M. Holl, et al., Phys. Lett. 795 (2019) 682.
[12] N.T. Toan Phuc, K. Yoshida, K. Ogata, Phys. Rev. C 100 (2019) 064604.
[13] A. Mecca, E. Cravo, A. Deltuva, R. Crespo, A.A. Cowley, A. Arriaga, R.B. Wiringa, T. Noro, Phys. Lett. B 798 (2019) 134989.
[14] R. Crespo, E. Cravo, A. Deltuva, Phys. Rev. C 99 (2019) 054622.
[15] R. Crespo, A. Arriaga, R. Wiringa, E. Cravo, A. Deltuva, A. Mecca, Phys. Lett. B 803 (2020) 135355.
[16] C.A. Bertulani, A. Idini, C. Barbieri, Phys. Rev. C 104 (2021) L061602.
[17] T. Aumann, C. Barbieri, D. Bazin, C.A. Bertulani, A. Bonaccorso, W.H. Dickhoff, A. Gade, M. Gómez-Ramos, B.P. Kay, A.M. Moro, T. Nakamura, A. Obertelli, K. Ogata, S. Paschalis, T. Uesaka, Prog. Part. Nucl. Phys. 118 (2021) 103847.
[18] I. Brida, Steven C. Pieper, R.B. Wiringa, Phys. Rev. C 84 (2011) 024319.
[19] R.B. Wiringa, Steven C. Pieper, Phys. Rev. Lett. 89 (2002) 182501.
[20] R.B. Wiringa, R. Schiavilla, Steven C. Pieper, J. Carlson, Phys. Rev. C 89 (2014) 024305.
[21] J. Carlson, et al., Rev. Mod. Phys. 87 (2015) 1067.
[22] R.B. Wiringa, Phys. Rev. C 73 (2006) 034317.
[23] S. Cohen, D. Kurath, Nucl. Phys. A 101 (1967) 1;
D. Kurath, private communication.
[24] www.phy.anl.gov/theory/research/overlaps.
[25] A. Lovato, I. Bombaci, D. Logoteta, M. Piarulli, R.B. Wiringa, Phys. Rev. C 105 (2022) 055808.
[26] M. Piarulli, A. Baroni, L. Girlanda, A. Kievsky, A. Lovato, Ewing Lusk, L.E. Marcucci, Steven C. Pieper, R. Schiavilla, M. Viviani, R.B. Wiringa, Phys. Rev. Lett. 120 (2018) 052503.
[27] Baroni, et al., Phys. Rev. C 98 (2018) 044003.
[28] M. Piarulli, S. Pastore, R.B. Wiringa, S. Brusilow, R. Lim, Phys. Rev. C 107 (2023) 014314.
[29] I. Sick, Phys. Lett. B 576 (2003) 62.
[30] P. Mueller, et al., Phys. Rev. Lett. 99 (2007) 252501.
[31] B. Maaß, et al., Phys. Rev. Lett. 122 (2021) 182501.
[32] H. De Vries, C.W. De Jager, C. De Vries, At. Data Nucl. Data Tables 36 (1987) 495.
[33] Z.-T. Lu, et al., Rev. Mod. Phys. 85 (2013) 1383.
[34] O. Jensen, et al., Phys. Rev. Lett. 107 (2011) 032501.
[35] C. Barbieri, W.H. Dickhoff, Int. J. Mod. Phys. A 24 (11) (2009) 2060.
[36] M.C. Atkinson, W.H. Dickoff, Phys. Lett. B 798 (2019) 135027.

[37] L.D. Faddeev, Zh. Eksp. Teor. Fiz. 39 (1960) 1459.
[38] E.O. Alt, P. Grassberger, W. Sandhas, Nucl. Phys. B 2 (1967) 167.
[39] V.R. Pandharipande, I. Sick, P.K.A. deWitt Huberts, Rev. Mod. Phys. 69 (1997).
[40] E. Caurier, G. Martınez-Pinedo, F. Nowacki, A. Poves, A.P. Zuker, Rev. Mod. Phys. 77 (2005) 427.
[41] A.J. Koning, J.P. Delaroche, Nucl. Phys. A 713 (2003) 231.
[42] E.D. Cooper, et al., Phys. Rev. C 47 (1993) 297.
[43] N. Kumar, Nucl. Phys. A 225 (1973) 221.
[44] A.E.L. Dieperink, T. de Forest Jr., Phys. Rev. C 10 (1974) 543.